

New Constraints on Lorentz Invariance Violation at High Redshifts from Multiband of GRBs

Mingyue Chen,¹ Yu Pan,^{1,*} Tonghua Liu,² and Shuo Cao^{3,†}

¹*College of Science, Chongqing University of Posts and Telecommunications, Chongqing 400065, China.*

²*School of Physics and Optoelectronic Engineering, Yangtze University, Jingzhou, 434023, China.*

³*Department of Astronomy, Beijing Normal University, Beijing 100875, China.*

(Dated: December 11, 2024)

In the gravity quantum theory, the quantization of spacetime may lead to the modification of the dispersion relation between the energy and the momentum and the Lorentz invariance violation (LIV). High energy and long-distance gamma-ray bursts (GRBs) observations in the universe provide a unique opportunity to test the possibility of LIV. In this paper, by using 93 time delay GRBs covering the redshift range of $0.117 < z < 6.29$, we present a new idea of using cosmological model-independent (based on the luminosity distance data from 174 GRBs) to test the LIV. Combining the observation data from multiband of GRBs provides us with an opportunity to mitigate the potential systematic errors arising from variations in the physical characteristics among diverse object populations, and to add a higher redshift dataset for testing the energy-dependent velocity caused by the corrected dispersion relationship of photons. These robust limits of the energy scale for the linear and quadratic LIV effects are $E_{QG,1} \geq 1.40 \times 10^{15}$ GeV, and $E_{QG,2} \geq 8.18 \times 10^9$ GeV, respectively. It exhibits a significantly reduced value compared to the energy scale of Planck in both scenarios of linear and quadratic LIV.

I. INTRODUCTION

To better explain the microstructure and basic physical laws of the universe, quantum gravity theory combines relativity with quantum mechanics [1]. The theory of quantum gravity states that space-time presents a discontinuous foam structure at the Planck scale, $E_{QG} \approx E_{PI} = \sqrt{\hbar c^5/G} \simeq 1.22 \times 10^{19}$ GeV, and that the foam structure could potentially be subject to interaction from high-energy photons [2, 3]. Lorentz invariance, a fundamental theorem in special relativity, argues the preservation of physical laws under Lorentz transformations, unveiling the inherent symmetry of spacetime. However, the interaction of the space-time bubble structure with high-energy photons causes the speed of light to change, which is contrary to the Lorentz invariance, a phenomenon known as Lorentz invariance violation (LIV) [1, 2]. Hence, the velocities of photons with different energies exhibit a bias, indicating that photons emitted from the same source but with varying energies do not arrive at the observer simultaneously. Measurement of the speed of light in a vacuum will help us to test the LIV. High-precision cosmology provides us with an opportunity to validate these theories, such as gravitational waves, ultra-high-energy cosmic rays, and neutrinos [4]. This paper focuses on the time delay of the GRBs [5–11].

Gamma-ray bursts (GRBs) are considered one of the farthest sources of gamma-ray emissions, and they are usually classified into two types based on their durations, with long and short GRBs [12]. Long GRBs are typically linked to core-collapse SN [13], while short GRBs are related to neutron star mergers [14]. In ad-

dition to the two types of GRBs mentioned above, several studies have proposed other subcategories [15, 16]. Because of the high-energy photons and the subsecond timescale variation on signal, GRBs are referred to as potential candidates for LIV investigations [17, 18]. Before the Fermi, some teams tested the LIV based on GRBs observations such as the Burst And Transient Source Experiment (BATSE) GRBs, GRB021206 from the Reuven Ramaty High Energy Solar Spectroscopic Imager (RHESSI), Swift, Konus-Wind and the High Energy Transient Explorer (HETE-2) [5, 6, 19–22]. Fermi observations get more stringent constraints on LIV, due to the exceptional sensitivity of the Fermi Large Area Telescope (LAT) in detecting high-energy GRBs emission (reaching up to tens of GeV). These constraints have been derived by the Fermi Collaboration based on their analysis of GRB080916C [23] and GRB090510 [24], as well as by [25] using data from GRB090510.

Most early studies of LIV were reliant on cosmological models, and the model parameters are out of consideration. Some works take the cosmological model parameters as a prior, while others consider the correlation between the cosmological model parameters and the LIV model parameters [7], treating the cosmological model parameters as free parameters. Additionally, some articles investigate the influence of cosmological models on LIV and show that the result is insensitive to the chosen cosmological model [7, 26]. Subsequently, some studies considered model-independent constraints on LIV [27, 28]. [27] used the luminosity distance (an associated measure of the cosmic expansion) of the Taylor series expansion, to calculate the time delay caused by the LIV. [28] proposed an alternative model-independent method to constraint LIV based on calibrating with the $H(z)$. And they reconstruct the history of the universe's expansion (using the Hubble parameter $H(z)$) by the Gaussian Process (GP), and fitted the dispersion relationship

* panyu@cqupt.edu.cn

† caoshuo@bnu.edu.cn

of high-energy photons by combining redshift matching with 23 GRBs time delay data in the redshift range of $0.165 < z < 2.5$. The time delay data sample of GRBs mentioned in the paper [28] has a redshift reaching 4.3. However, due to the maximum redshift value of $H(z)$ being 2.5, any delay data with a redshift greater than 2.5 is excluded. Ultimately, the prescribed lower limit for the energy scale is $E_{QG,1} \geq 0.3 \times 10^{15}$ GeV and $E_{QG,2} \geq 0.6 \times 10^9$ GeV.

In this study, building upon the framework proposed by [28], we present a novel approach for model-independent constraint on LIV, and validate this method based on a dataset comprising 93 temporal delay data points. On the one hand, we reconstruct the cosmic expansion history using luminosity distance information from 174 GRBs calibrated by [29], the redshift range is $0.117 < z < 9.4$. On the other hand, the observed time delay data are provided by multi-observation GRBs we collected [30–35], with a total dataset of 93, covering a redshift range from 0.117 to 6.29. Compared to the approach of [28], which reconstructed the cosmic expansion history using $H(z)$ data, the cosmic expansion history information and time-delay information utilized in this paper are exclusively derived from GRBs. That could potentially mitigate systematic errors arising from variations in the physical characteristics among diverse object populations. Furthermore, the luminosity distance data here encompasses a wide redshift range, allowing for the inclusion of more time-delay information. In comparison to [28], it boasts a larger dataset and an increased upper redshift limit for the samples, reaching up to $z = 6.29$.

This paper is structured as follows: In Section II we describe a simple derivation of the time delay caused by LIV. Section III will introduce the methods and datasets used in the study, encompassing time delay data, luminosity distance data, and the Gaussian Process regression reconstruction method. In section IV, we will unveil the conclusive outcomes. The concluding section shall encompass a concise overview and final remarks for this article.

II. TIME DELAY OF LORENTZ INVARIANCE VIOLATION

Quantum gravity theories suggest that Lorentz invariance may be broken at the Planck energy scale $E_{QG} \sim 10^{19}$ GeV. One of the phenomena associated with this is a potential alteration in the speed of light, and the dispersion equation for photons is expressed as follows:

$$E^2 = p^2 c^2 [1 - s_{\pm} (\frac{E}{E_{QG}})^n]. \quad (1)$$

In this context, the E and p denote the energy and momentum of photons, respectively. The energy scale denoted as E_{QG} corresponds to the Planck energy. The variables s_{\pm} take values of ± 1 , and when $s_{\pm} = 1$, the speed of light decreases with increasing energy; when $s_{\pm} = -1$, the energy increase leads to a reduction in

the speed of light. In this work, we set the $s_{\pm} = 1$, indicating that the speed of light is inversely proportional to energy. The parameter n represents the order of the vacuum dispersion relation, when n equals 1 or 2, it represents linear and quadratic relationships, respectively.

The relationship between the speed of light and energy can be expressed as:

$$v(E) = c [1 - s_{\pm} \frac{n+1}{2} (\frac{E}{E_{QG}})^n]. \quad (2)$$

The speed discrepancy between high-energy and low-energy photons accumulates during the process of photon propagation, and the time delay induced by LIV is ultimately obtained. The time delay between high-energy and low-energy photons caused by LIV can be written

$$\Delta t_{LIV} = -\frac{1+n}{2H_0} \frac{E^n - E_0^n}{E_{QG,n}^n} \int_0^z \frac{(1+z')^n dz'}{h(z')}, \quad (3)$$

where $h(z) = H(z)/H_0$, $H(z)$ is the Hubble parameter and H_0 is the Hubble function's current value. We order that

$$K(z) = \int_0^z \frac{(1+z')^n dz'}{h(z')}, \quad (4)$$

the $K(z)$ is the term in the time delay expression (Δt_{LIV}) induced by LIV associated with the cosmological model. In this paper, we reconstruct $K(z)$ from the luminosity distance of the calibrated 174 GRBs, avoiding the use of cosmological models.

In addition to the time delay caused by photon vacuum scattering, the observed time delay should also include the time delay of the emission time of photons of different energies when GRBs are emitted. [6] first attempted to alleviate the inherent time delay issue, in their work, the intrinsic time delay is taken as a constant. Subsequently, [8] no longer regard the inherent time delay as a constant, and assume the intrinsic positive time lag (between the lowest energy band and any other high-energy bands) increases with the energy E in the form of an approximate power-law function. Here Δt_{int} is the intrinsic time delay:

$$\Delta t_{int} = \tau [(\frac{E}{KeV})^{\alpha} - (\frac{E_0}{KeV})^{\alpha}]. \quad (5)$$

The median value of the lowest energy band, denoted as E_0 , is considered along with two free parameters τ and α . When $\tau > 0$ and $\alpha > 0$, the inherent time delay is positive.

The total time delay can be affected by many factors, in this paper, we only consider the time delay caused by LIV Δt_{LIV} , and inherent time delay Δt_{int} , so we consider E_{QG} as a statistically robust lower limit,

$$\Delta t = \Delta t_{LIV} + \Delta t_{int}(1+z). \quad (6)$$

III. DATA-SET OF GRBS AND MODEL-INDEPENDENT METHODS

III.1. Data-set of GRBs

In this paper, we implement cosmological model-independent constraints for LIV via multiband GRBs observations. First, we collect 93 time delay data of GRBs from different observations. Later, we reconstructed $K(z)$ from the luminosity distance data of 174 GRBs calibrated by [29]. by a cosmological model-independent method.

In this work, we utilized 93 time delay data of GRBs obtained from different observations, the redshift range is $0.017 < z < 6.29$. There are 37 datasets from the observation of GRB160625B by the Fermi Gamma-Ray Burst Monitor (GBM) and the Fermi LAT [30, 31]. GRB160625B consists of three sub-bursts, with a total duration of 770 seconds [32]. Its brightness during the second burst was of such intensity that it facilitated the extraction of its light curves across various energy ranges. [8] calculated the time delay between light curves of different energies by using the cross-correlation function (CCF [33]) method. They also recorded the time delay between the light curve in the energy range of $10 \sim 12$ KeV and other light curves at higher energies (refer to Table 1 in [8]). Also include the 35 datasets from Table 1 in [34], with 9 being identified through observations obtained by BATSE, another 15 captured by the HETE satellite, and an additional 11 recorded via the Swift satellite. They searched for spectral time lags in the range of $115 \sim 320$ KeV to $25 \sim 55$ KeV in the publicly available light curve data. And there are 21 from Table 3 provided in reference [35], obtained by GBM, and Swift. They recorded spectral time lags between the low-energy band of $15 \sim 70$ KeV and the high-energy band of $120 \sim 250$ KeV, within a redshift range of $0.117 < z < 2.938$.

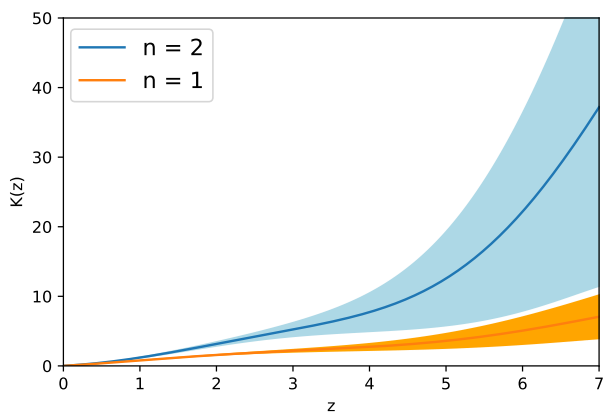


FIG. 1. Distribution of reconstructed $K(z)$ with redshifts, in the two cases of $n = 1$ and $n = 2$.

The 174 luminosity distance data we used is calibrated

by [29], by a cosmological model-independent method, which is a complete gamma-ray and X-ray data set filtered from Swift satellite. And the redshift range of this sample is $0.117 < z < 9.4$. Luminosity distance can be obtained by the GRBs correlation proposed by [36], which is called the Combo-relation. The Combo-relation is,

$$\log\left(\frac{L_0}{\text{erg/s}}\right) = \log\left(\frac{A}{\text{erg/s}}\right) + \gamma \log\left(\frac{E_{p,i}}{\text{KeV}}\right) - \log\left(\frac{\tau_c/s}{|1 + \alpha_c|}\right), \quad (7)$$

where, the log represents the base-10 logarithm, L_0 signifies the isotropic equivalent luminosity during the plateau phase, γ and A correspond to the gradient and intercept parameters respectively, $E_{p,i}$ denotes the peak energy of the νF_ν spectrum in the rest frame, α_c and τ_c stands for the decay index during the later power-law phase and the characteristic timescale at the end of the plateau, respectively. When provided with the luminosity distance of a given GRB, the luminosity L_0 during the plateau phase can be deduced from the energy flux F_0 in the rest-frame $0.3 \sim 10$ keV range.

$$L_0 = 4\pi D_L^2 F_0, \quad (8)$$

the luminosity distance D_L is interconnected with the distance modulus μ (which is a dimensionless quantity), through a certain relationship:

$$\mu = 5 \log \frac{D_L}{\text{Mpc}} + 25. \quad (9)$$

The distance modulus associated with GRBs [29, 36, 37].

$$\mu_{GRB} = -97.45 + \frac{5}{2} [\log(A) + \gamma \log(E_{p,i}) - \log\left(\frac{\tau_c}{|1 + \alpha_c|}\right) - \log(F_0) - \log 4\pi]. \quad (10)$$

where A , γ and δ_{GRB} are all free parameters.

[29] trained a neural network with the Pantheon compilation of Type-Ia supernovae, and they used the trained neural network to calibrate 174 GRBs of [37], giving the values of the free parameters, $\gamma = 0.856$, $\log A = 49.661$, $\delta_{GRB} = 0.228$. In our paper, we omit this step and directly utilize the results obtained by [29].

III.2. Methods

To implement the cosmological model-independent LIV restriction, we need to replace $h(z)$ in $K(z)$; therefore, we reconstruct the $K(z)$ with luminosity distance data from GRBs calibrated by [29]. The expression for the luminosity distance in a flat universe can be written as

$$D_L(z) = \frac{c(1+z)}{H_0} \int_0^z \frac{dz'}{h(z')}, \quad (11)$$

where c is the speed of light and H_0 is the Hubble constant, here we take $H_0 = 70$ km/s/Mpc.

After a simple transformation of the equation, the derivative of $K(z)$ can be expressed as:

$$\frac{dK(z)}{dz} = \frac{(1+z)^n}{h(z)} = \frac{d(\frac{H_0}{c(1+z)}D_L)}{dz}(1+z)^n \quad (12)$$

the value of $dK(z)/dz$ has been calculated from D_L given by the "Combo relation". They are discrete data points with redshift z plotted on the x-axis and $dK(z)/dz$ on the y-axis. By approximately integrating these discrete points, we finally obtain the discrete points of $K(z)$.

It is worth noting that when we apply both the time delay data and the reconstructed $K(z)$, we should match the redshift z of the two data sets to each other. By the GP method [38], the 174 scattered luminosity distance D_L (obtained by 174 GRBs) can be augmented to approximately continuous scattered points on the z-axis. The GP is entirely data-driven, independent of cosmological models. Holsclaw was the first one to use this reconstruction method in supernova measurements, and subsequently [39], GP has also been applied in cosmological research [40–43].

The reconstructed $K(z)$ is shown in Fig. 1. The $K(z)$ reconstruction is driven entirely by the luminosity distance data from the 174 GRBs and is independent of the cosmological model.

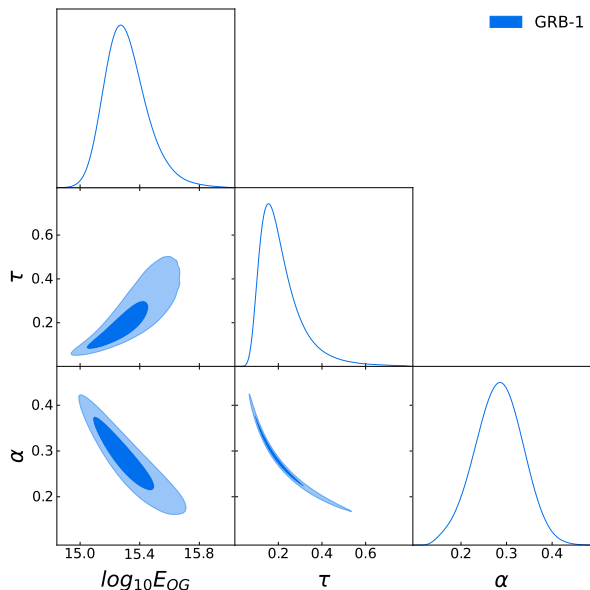


FIG. 2. The individual probability distribution of each parameter and the confidence contours in two dimensions for the parameters E_{QG} , τ , and α in 1σ (considering linear LIV scenario with $n = 1$), the light is the 68% contour, and the dark is the 95% contour.

TABLE I. The 1σ Bounds on E_{QG} , τ , and α for Various LIV Models ($n = 1$, $n = 2$)

Model parameter	$n = 1$	$n = 2$
$\log E_{QG}$	$15.358^{+0.069}_{-0.210}$	$9.973^{+0.049}_{-0.060}$
τ	$0.228^{+0.025}_{-0.13}$	$0.312^{+0.056}_{-0.140}$
α	$0.280^{+0.059}_{-0.050}$	$0.225^{+0.038}_{-0.038}$

IV. RESULTS AND DISCUSSION

The Markov chain Monte Carlo (MCMC) method is employed in this paper to constrain the pertinent parameters ($\log E_{QG}$, τ , α). Its parameters range as: [7, 23], [0.005, 2], and [0.01, 1.5], with uniform prior probability distributions set within these ranges. Now, by replacing the cosmological model with the reconstructed $K(z)$, the log likelihood expressed as follows:

$$\text{Loglikelihood} = \sum_{i=1}^n \left[\frac{\Delta t_{obs} - \Delta t_{th}(E_{QG}, \tau, \alpha)}{\sigma_{tot}} \right]^2. \quad (13)$$

Where Δt_{obs} can be directly obtained from the time delay datasets, Δt_{th} is derived from the theoretical expression for time delay derived from the reconstructed $K(z)$, and (E_{QG}, τ, α) represent the unknown parameters that we need to fit. σ_{tot} represents the total error, and it is equal to:

$$\sigma_{tot}^2 = \sigma_t^2 + \left(\frac{\partial f}{\partial E} \right)^2 \sigma_E^2 + \left(\frac{\partial f}{\partial E_0} \right)^2 \sigma_{E_0}^2 + \sigma_{D_L}^2. \quad (14)$$

In this equation, f represents the specific model; σ_t indicates the uncertainty in spectral lag; σ_{E_0} and σ_E represent the widths of the lower and upper energy intervals respectively. The σ_{D_L} represents the error from luminosity distance data.

To ensure convergence of results, we set the chain length to 300,000. This article investigates time delays in linear and quadratic relationships, corresponding to $n = 1$ and $n = 2$, respectively. The fitting results with a confidence interval of 1σ (68%) are presented in Table I.

We initially fitted the lag energy in 1σ under linear conditions ($n = 1$). Fig. 2 is a two-dimensional density plot illustrating the fitting results when $n = 1$. And the best-fit parameter values are $\log E_{QG} = 15.358^{+0.069}_{-0.210}$, $\tau = 0.228^{+0.025}_{-0.130}$ and $\alpha = 0.280^{+0.059}_{-0.050}$.

Then we consider the quadratic case in 1σ which $n = 2$. The parametric results of the constraints are shown in Fig. 3. The best-fit parameter values are $\log E_{QG} = 9.973^{+0.049}_{-0.060}$, $\tau = 0.312^{+0.056}_{-0.140}$ and $\alpha = 0.225^{+0.038}_{-0.038}$.

With the best-fit values of $\log E_{QG,1}$ and $\log E_{QG,2}$ as well as their 1σ error bars, the 1σ confidence-level lower limit on LIV is $E_{QG,1} \geq 1.40 \times 10^{15}$ GeV and $E_{QG,2} \geq 8.18 \times 10^9$ GeV. The $E_{QG,1}$ is reduced by four orders of magnitude compared to the Planck energy, and the energy $E_{QG,2}$ is significantly smaller than the Planck energy by a factor of ten orders of magnitude. In the linear case, our results are slightly lower than those of

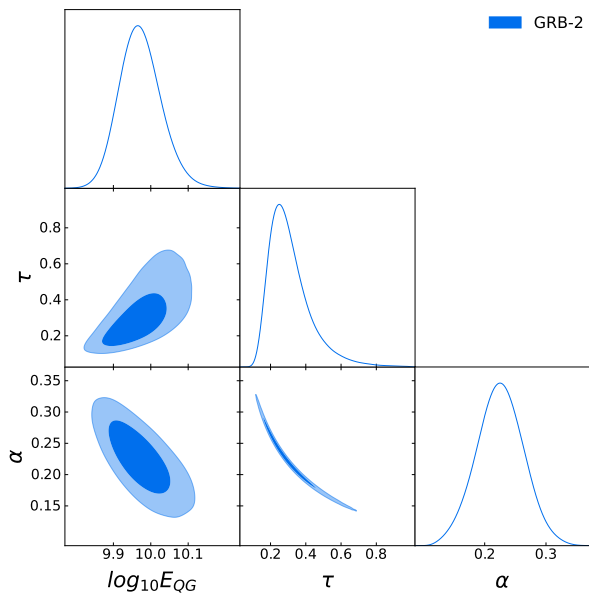


FIG. 3. The individual probability distribution of each parameter and the confidence contours in two dimensions for the parameters E_{QG} , τ , and α in 1σ (considering quadratic LIV scenario with $n = 2$), the light is the 68% contour, and the dark is the 95% contour.

[6] and [8]. When $n=2$, our result is nearly three orders of magnitude higher than the result of [8]. In comparison with [28], the obtained lower bound of $E_{QG,1}$ in the linear scenario is elevated by an order of magnitude, and the result in the quadratic scenario is also raised by approximately one order of magnitude. [35] calculated $E_{QG,1} \geq 2.5 \times 10^{15}$ GeV and $E_{QG,2} \geq 1.2 \times 10^6$ GeV separately, which considered constant intrinsic time delays using 46 SRGBs, providing a level of credibility to the enhanced delay model. In the linear case ($n = 1$), the result is consistent with ours. In terms of constraint accuracy, our quadratic result is significantly higher than [8], but the linear result is lower than their results. Although our results are somewhat lower in precision than the previous ones, this approach may potentially circumvent unknown discrepancies among various cosmological probes. The best fit value $\tau = 0.228_{-0.130}^{+0.025}$, $\alpha = 0.280_{-0.050}^{+0.059}$ in our work, when $n = 1$. And when $n = 2$, $\tau = 0.312_{-0.140}^{+0.056}$, $\alpha = 0.225_{-0.038}^{+0.038}$. The parameter $\tau > 0$ and $\alpha > 0$ indicates that the intrinsic time-lags are positive, suggesting a forward directionality, and time delay and photon energy are positively correlated. In comparison to the results obtained by [8], our results give smaller intrinsic time delays.

From the results above, it appears that our findings in line with those of similar studies, given the relatively small differences in data samples. This lends a degree of confirmation to the validity of our work. In higher-energy data samples, [9] previously reported an E_{QG} constraint result of 7.6 times the Planck value based on the GRB091510, which is four orders of magnitude higher than our findings.

V. CONCLUSION

In this study, we apply a new cosmological model-independent restriction to LIV using time delay data and luminosity distance data from GRBs. Initially, we collected a dataset consisting of 93 time delay obtained from Multiple observations of GRBs, reaching the redshift to $z \sim 6.29$. Subsequently, we employ the GP methodology to reconstruct the luminosity distance datasets from 174 GRBs into $K(z)$. Additionally, the power-law model of inherent time delays is incorporated in our LIV model, with two parameters τ and α .

Under the constraints of multiband GRBs, we get the LIV limit results at higher redshifts ($0.117 < z < 6.29$), the linear and quadratic LIV effects are $E_{QG,1} \geq 1.4 \times 10^{15}$ and $E_{QG,2} \geq 8.18 \times 10^9$. The magnitude exhibits a significant reduction in comparison to the energy scale of Planck. With the support of the 93 time delay dataset from multi-observation GRBs, we obtain the relatively accurate intrinsic time delay constraint: $\tau = 0.228_{-0.130}^{+0.025}$ and $\alpha = 0.280_{-0.050}^{+0.059}$ ($n = 1$), $\tau = 0.312_{-0.140}^{+0.056}$ and $\alpha = 0.225_{-0.038}^{+0.038}$ ($n = 2$). In our results, the intrinsic time delay is positive and proportional to the energy of the photon. All of the results are consistent with the previous studies. We combine the luminosity distance with the time delay information used in this paper, which comes entirely from GRBs. This might alleviate some systematics coming from different physical properties of different populations of objects, providing a more compelling set of constraints.

In a word, we present a novel approach to constrain LIV independent of cosmological models. To achieve tighter LIV constraints, the support from a larger number of GRBs time delay data with enhanced accuracy and higher energy band is anticipated in our study. Combined with more observations, we may be able to further investigate the constraints of LIV and explore the underlying physics behind LIV.

ACKNOWLEDGMENTS

This work was supported by National Natural Science Foundation of China Grant No. 12105032.

[1] G. Amelino-Camelia, Quantum-Spacetime Phenomenology, Living Rev. Rel. **16**, 5 (2013), arXiv:0806.0339 [gr-qc].

[2] G. Amelino-Camelia, J. R. Ellis, N. E. Mavromatos, and D. V. Nanopoulos, Distance measurement and wave dispersion in a Liouville string approach to quantum grav-

- ity, *Int. J. Mod. Phys. A* **12**, 607 (1997), arXiv:hep-th/9605211.
- [3] D. Mattingly, Modern tests of Lorentz invariance, *Living Rev. Rel.* **8**, 5 (2005), arXiv:gr-qc/0502097.
- [4] A. Addazi *et al.*, Quantum gravity phenomenology at the dawn of the multi-messenger era—A review, *Prog. Part. Nucl. Phys.* **125**, 103948 (2022), arXiv:2111.05659 [hep-ph].
- [5] J. R. Ellis, N. E. Mavromatos, D. V. Nanopoulos, and A. S. Sakharov, Quantum-gravity analysis of gamma-ray bursts using wavelets, *Astron. Astrophys.* **402**, 409 (2003), arXiv:astro-ph/0210124.
- [6] J. R. Ellis, N. E. Mavromatos, D. V. Nanopoulos, A. S. Sakharov, and E. K. G. Sarkisyan, Robust limits on Lorentz violation from gamma-ray bursts, *Astropart. Phys.* **25**, 402 (2006), [Erratum: *Astropart. Phys.* **29**, 158–159 (2008)], arXiv:0712.2781 [astro-ph].
- [7] Y. Pan, Y. Gong, S. Cao, H. Gao, and Z.-H. Zhu, Constraints on the Lorentz Invariance Violation With Gamma-ray Bursts via a Markov Chain Monte Carlo Approach, *Astrophys. J.* **808**, 78 (2015), arXiv:1505.06563 [astro-ph.CO].
- [8] J.-J. Wei, B.-B. Zhang, L. Shao, X.-F. Wu, and P. Mészáros, A New Test of Lorentz Invariance Violation: the Spectral Lag Transition of GRB 160625B, *Astrophys. J. Lett.* **834**, L13 (2017), arXiv:1612.09425 [astro-ph.HE].
- [9] V. Vasileiou, A. Jacholkowska, F. Piron, J. Bolmont, C. Couturier, J. Granot, F. W. Stecker, J. Cohen-Tanugi, and F. Longo, Constraints on Lorentz Invariance Violation from Fermi-Large Area Telescope Observations of Gamma-Ray Bursts, *Phys. Rev. D* **87**, 122001 (2013), arXiv:1305.3463 [astro-ph.HE].
- [10] S. Zhang and B.-Q. Ma, Lorentz violation from gamma-ray bursts, *Astroparticle Physics* **61**, 108 (2015), arXiv:1406.4568 [hep-ph].
- [11] K. Liao, M. Biesiada, and Z.-H. Zhu, Strongly Lensed Transient Sources: A Review, *Chin. Phys. Lett.* **39**, 119801 (2022), arXiv:2207.13489 [astro-ph.HE].
- [12] C. Kouveliotou, C. A. Meegan, G. J. Fishman, N. P. Bhyat, M. S. Briggs, T. M. Koshut, W. S. Paciesas, and G. N. Pendleton, Identification of two classes of gamma-ray bursts, *Astrophys. J. Lett.* **413**, L101 (1993).
- [13] S. E. Woosley and J. S. Bloom, The Supernova Gamma-Ray Burst Connection, *Ann. Rev. Astron. Astrophys.* **44**, 507 (2006), arXiv:astro-ph/0609142.
- [14] E. Nakar, Short-Hard Gamma-Ray Bursts, *Phys. Rept.* **442**, 166 (2007), arXiv:astro-ph/0701748.
- [15] S. Kulkarni and S. Desai, Classification of Gamma-Ray Burst durations using robust model-comparison techniques, *Astrophys. Space Sci.* **362**, 70 (2017), arXiv:1612.08235 [astro-ph.HE].
- [16] A. Bhave, S. Kulkarni, S. Desai, and P. K. Srijith, Two dimensional clustering of Gamma-Ray Bursts using durations and hardness, *Astrophys. Space Sci.* **367**, 39 (2022), arXiv:1708.05668 [astro-ph.IM].
- [17] J.-J. Wei and X.-F. Wu, Testing fundamental physics with astrophysical transients, *Front. Phys.* **16**, 44300 (2021), arXiv:2102.03724 [astro-ph.HE].
- [18] R. Agrawal, H. Singirikonda, and S. Desai, Search for Lorentz Invariance Violation from stacked Gamma-Ray Burst spectral lag data, *JCAP* **05**, 029, arXiv:2102.11248 [astro-ph.HE].
- [19] S. E. Boggs, C. B. Wunderer, K. Hurley, and W. Coburn, Testing Lorentz non-invariance with GRB021206, *Astrophys. J. Lett.* **611**, L77 (2004), arXiv:astro-ph/0310307.
- [20] M. Rodriguez Martinez, T. Piran, and Y. Oren, Grb 051221a and tests of Lorentz symmetry, *JCAP* **05**, 017, arXiv:astro-ph/0601556.
- [21] J. Bolmont, A. Jacholkowska, J. L. Atteia, F. Piron, and G. Pizzichini, Study of time lags in HETE-2 Gamma-Ray Bursts with redshift: search for astrophysical effects and Quantum Gravity signature, *Astrophys. J.* **676**, 532 (2008), arXiv:astro-ph/0603725.
- [22] R. Lamon, N. Produit, and F. Steiner, Study of Lorentz violation in INTEGRAL gamma-ray bursts, *Gen. Rel. Grav.* **40**, 1731 (2008), arXiv:0706.4039 [gr-qc].
- [23] A. A. Abdo *et al.* (Fermi-LAT, Fermi GBM), Fermi Observations of High-Energy Gamma-Ray Emission from GRB 080916C, *Science* **323**, 1688 (2009).
- [24] M. Ackermann *et al.* (Fermi GBM/LAT), A limit on the variation of the speed of light arising from quantum gravity effects, *Nature* **462**, 331 (2009), arXiv:0908.1832 [astro-ph.HE].
- [25] Z. Xiao and B.-Q. Ma, Constraints on Lorentz invariance violation from gamma-ray burst GRB090510, *Phys. Rev. D* **80**, 116005 (2009), arXiv:0909.4927 [hep-ph].
- [26] M. Biesiada and A. Piorowska, Lorentz invariance violation-induced time delays in GRBs in different cosmological models, *Class. Quant. Grav.* **26**, 125007 (2009), arXiv:1008.2615 [astro-ph.CO].
- [27] X.-B. Zou, H.-K. Deng, Z.-Y. Yin, and H. Wei, Model-Independent Constraints on Lorentz Invariance Violation via the Cosmographic Approach, *Phys. Lett. B* **776**, 284 (2018), arXiv:1707.06367 [gr-qc].
- [28] Y. Pan, J. Qi, S. Cao, T. Liu, Y. Liu, S. Geng, Y. Lian, and Z.-H. Zhu, Model-independent constraints on Lorentz invariance violation: implication from updated Gamma-ray burst observations, *Astrophys. J.* **890**, 169 (2020), arXiv:2001.08451 [astro-ph.CO].
- [29] L. Tang, H.-N. Lin, X. Li, and L. Liu, Reconstructing the Hubble diagram of gamma-ray bursts using deep learning, *Mon. Not. Roy. Astron. Soc.* **509**, 1194 (2021), arXiv:2111.10052 [gr-qc].
- [30] E. Burns, GRB 160625B: Fermi GBM initial observations., *GRB Coordinates Network* **19581**, 1 (2016).
- [31] F. Dirirsa, J. Racusin, J. McEnery, and R. Desiante, GRB 160625B: Fermi-LAT detection of a bright burst., *GRB Coordinates Network* **19580**, 1 (2016).
- [32] B. B. Zhang *et al.*, Transition from fireball to Poynting-flux-dominated outflow in the three-episode GRB 160625B, *Nature Astron.* **2**, 69 (2018), arXiv:1612.03089 [astro-ph.HE].
- [33] B.-B. Zhang, D. N. Burrows, B. Zhang, P. Mészáros, X.-Y. Wang, G. Stratta, V. D’Elia, D. Frederiks, S. Golenetskii, J. R. Cummings, J. P. Norris, A. D. Falcone, S. D. Barthelmy, and N. Gehrels, Unusual Central Engine Activity in the Double Burst GRB 110709B, *Astrophys. J.* **748**, 132 (2012), arXiv:1111.2922 [astro-ph.HE].
- [34] J. Ellis, N. E. Mavromatos, D. V. Nanopoulos, A. S. Sakharov, and E. K. G. Sarkisyan, Robust limits on Lorentz violation from gamma-ray bursts, *Astroparticle Physics* **25**, 402 (2006), arXiv:astro-ph/0510172 [astro-ph].
- [35] S. Xiao *et al.*, A Robust Estimation of Lorentz Invariance Violation and Intrinsic Spectral Lag of Short Gamma-Ray Bursts, *Astrophys. J. Lett.* **924**, L29 (2022).
- [36] L. Izzo, M. Muccino, E. Zaninoni, L. Amati, and M. Della Valle, New measurements of Ω_m from gamma-ray bursts, *Astron. Astrophys.* **582**, A115 (2015), arXiv:1508.05898 [astro-ph.CO].

- [37] M. Muccino, L. Izzo, O. Luongo, K. Boshkayev, L. Amati, M. Della Valle, G. B. Pisani, and E. Zaninoni, Tracing dark energy history with gamma ray bursts, *Astrophys. J.* **908**, 181 (2021), arXiv:2012.03392 [astro-ph.CO].
- [38] M. Seikel, C. Clarkson, and M. Smith, Reconstruction of dark energy and expansion dynamics using Gaussian processes, *JCAP* **06**, 036, arXiv:1204.2832 [astro-ph.CO].
- [39] T. Holsclaw, U. Alam, B. Sansó, H. Lee, K. Heitmann, S. Habib, and D. Higdon, Nonparametric Dark Energy Reconstruction from Supernova Data, *Phys. Rev. Lett.* **105**, 241302 (2010), arXiv:1011.3079 [astro-ph.CO].
- [40] S. Cao, J. Qi, M. Biesiada, X. Zheng, T. Xu, Y. Pan, and Z.-H. Zhu, Milliarcsecond compact structure of radio quasars and the geometry of the Universe, *Physics of the Dark Universe* **24**, 100274 (2019).
- [41] S. Cao, X. Zheng, M. Biesiada, J. Qi, Y. Chen, and Z.-H. Zhu, Ultra-compact structure in intermediate-luminosity radio quasars: building a sample of standard cosmological rulers and improving the dark energy constraints up to $z \sim 3$, *Astron. Astrophys.* **606**, A15 (2017), arXiv:1708.08635 [astro-ph.CO].
- [42] S. Cao, M. Biesiada, J. Qi, Y. Pan, X. Zheng, T. Xu, X. Ji, and Z.-H. Zhu, Cosmological investigation of multi-frequency VLBI observations of ultra-compact structure in $z \sim 3$ radio quasars, *European Physical Journal C* **78**, 749 (2018), arXiv:1708.08639 [astro-ph.CO].
- [43] J.-Z. Qi, S. Cao, S. Zhang, M. Biesiada, Y. Wu, and Z.-H. Zhu, The distance sum rule from strong lensing systems and quasars – test of cosmic curvature and beyond, *Mon. Not. Roy. Astron. Soc.* **483**, 1104 (2019), arXiv:1803.01990 [astro-ph.CO].
- [44] U. Jacob and T. Piran, Lorentz-violation-induced arrival delays of cosmological particles, *JCAP* **01**, 031, arXiv:0712.2170 [astro-ph].
- [45] D. Staicova, Impact of cosmology on Lorentz Invariance Violation constraints from GRB time-delays, *Class. Quant. Grav.* **40**, 195012 (2023), arXiv:2305.06504 [gr-qc].
- [46] P. Kumar and B. Zhang, The physics of gamma-ray bursts & relativistic jets, *Phys. Rept.* **561**, 1 (2014), arXiv:1410.0679 [astro-ph.HE].
- [47] A. Singh and S. Desai, Search for cosmological time dilation from gamma-ray bursts — a 2021 status update, *JCAP* **02** (02), 010, arXiv:2108.00395 [astro-ph.HE].